

Limits to phase resolution in matter wave interferometry.

M. Jääskeläinen¹, W. Zhang², and P. Meystre¹

¹ *Optical Sciences Center, The University of Arizona, AZ 85721 and*

² *Department of Physics, Tsinghua University, Beijing 100084, China*

(Dated: July 12, 2018)

We study the quantum dynamics of a two-mode Bose-Einstein condensate in a time-dependent symmetric double-well potential using analytical and numerical methods. The effects of internal degrees of freedom on the visibility of interference fringes during a stage of ballistic expansion are investigated varying particle number, nonlinear interaction sign and strength as well as tunneling coupling. Expressions for the phase resolution are derived and the possible enhancement due to squeezing is discussed. In particular, the role of the superfluid - Mott insulator cross-over and its analog for attractive interactions is recognized.

PACS numbers: 03.75.Be, 03.65.Ge, 05.60.Gg

I. INTRODUCTION

Coherent atom optics offers considerable promise for applications in a numbers of areas from precision measurements to rotation sensors, accelerometers, and gravity gradiometers [1, 2]. One key element in any practical device is a coherent beam splitter, and much effort has been devoted to the realization and the understanding of these devices, both experimentally [3, 4, 5] and theoretically [6, 7, 8, 9, 10, 11, 12, 13].

In contrast to light fields, which do not interact in a vacuum, matter waves are subject to collisions, mostly two-body interactions in the low density beams normally considered when using quantum-degenerate atomic systems. At extremely low temperatures, collisions produce a nonlinear phase shift of the matter waves that is proportional to the atomic density, and hence leads under normal conditions to undesirable phase noise [14]. This is a serious difficulty that needs to be addressed in detail. On the other hand, two-body collisions are also known to act as the matter-wave analog of a cubic nonlinearity in optics. As such, they can be used to generate nonclassical states of the Schrödinger field. These states can in turn be exploited to achieve phase resolution below the standard shot-noise limit.

The use of squeezing to reduce quantum noise was suggested in [15] for Ramsey-type interferometry. For optical Mach-Zender interferometry a Heisenberg limited scheme was outlined in [16], and related schemes using dual Fock-states were suggested for Bose-condensed atoms later. [17, 18, 19]. A scheme dependent on parity measurement was suggested in [20].

A matter-wave beam splitter can be thought of as a double-well potential with time-dependent well separation. At zero temperature, the dominant mechanism by which atoms move from one well to the other is quantum tunnelling. It is known that in quantum-degenerate bosonic systems, the interplay between tunnelling and collisions and the associated mean-field energy can result in highly non-trivial effects [21]. For instance, in the case of repulsive interactions a condensate trapped on a lattice potential can undergo a quantum phase transi-

tion from a superfluid state, characteristic of situations where tunneling is dominant, to a Mott insulator state, characteristic of situations where the mean-field energy dominates the dynamics [22, 23, 24]. The situation is more complicated in the case of attractive interactions, since the condensate is then unstable unless it is small enough to be stabilized by its kinetic energy [25]. Such small, stable condensates also undergo a transition reminiscent of the superfluid-Mott insulator transition in the sense that the ground state [26, 27] changes its statistical properties at a critical value of the interaction strength.

With these processes in mind, the goal of this paper is to assess in detail the limits in phase resolution of an atomic beam splitter under the combined effects of collision-driven cubic nonlinearities and quantum tunneling. The combination of these effects renders a full quantum-mechanical description of an atomic beam splitter highly non-trivial. Consequently, we restrict our discussion to a two-mode analysis, using a combination of numerical and analytical tools.

This paper is organized as follows: Section II discusses our model and establishes the notation. Section III A presents results of a numerical analysis of the static problem where the condensates are released from a beam splitter with fixed well separation. Depending upon the ratio of mean field energy to inter-well tunneling energy, the beam splitter operates either in the superfluid or Mott insulator-like regime, with qualitative and quantitative differences in their noise properties. For attractive interactions, the phase noise of the beam splitter is found to be significantly reduced at the transition between the two regimes. These results are extended to the dynamical regime in Section III B, which discusses in particular the departure of the system from adiabaticity. Finally, section IV is a summary and outlook.

II. MODEL

We consider in 1+1 dimensions the quantum dynamics of an ultracold bosonic atomic beam trapped in a double-well potential $V(y, d)$ with time-dependent well

separation $2d(t)$. A beam splitter using such a time-dependent configuration of optical waveguides has been realized by the MIT group [28], the resulting atomic field being detected after turning off the trap and ballistic free expansion of the atomic condensate. Assuming that the atomic density is low enough that we can neglect three-body collisions, the Hamiltonian of this system is

$$H = \int_{-\infty}^{\infty} dy \hat{\Psi}^\dagger(y) \left[-\frac{\hbar^2}{2M} \nabla^2 + V(y, d) \right] \hat{\Psi}(y) + g_2 \int_{-\infty}^{\infty} dy \hat{\Psi}^\dagger(y) \hat{\Psi}^\dagger(y) \hat{\Psi}(y) \hat{\Psi}(y), \quad (1)$$

where g_2 is the two-body coupling constant, taken to be negative for attractive two-body interactions. In the absence of excitations to higher spatial modes, the field operator $\hat{\Psi}(y)$ can be expanded into two modes corresponding to particles located around the two minima of the double-well potential as

$$\hat{\Psi}(y) = \varphi_L(y, d) \hat{a}_L + \varphi_R(y, d) \hat{a}_R. \quad (2)$$

Here $\hat{a}_{L(R)}$ are bosonic annihilation operators for the “left” and “right” mode of the matter-wave field, and $\varphi_{L(R)}$ are the corresponding spatial mode functions. For sufficiently harmonic potentials they can be approximated by

$$\varphi(y, d)_{L(R)} = \frac{1}{(\pi \Delta y^2)^{\frac{1}{4}}} \exp \left[-\frac{(y \pm d)^2}{4 \Delta y^2} \right], \quad (3)$$

the minus sign corresponding to $\varphi_R(y, d)$ and the plus sign to $\varphi_L(y, d)$. Within this two-mode approximation, the Hamiltonian (1) becomes

$$H(t) = \hbar \omega (\hat{a}_L^\dagger \hat{a}_L + \hat{a}_R^\dagger \hat{a}_R) + \frac{\Delta E(t)}{2} [\hat{a}_L^\dagger \hat{a}_R + \hat{a}_R^\dagger \hat{a}_L] + g [\hat{a}_L^{\dagger 2} \hat{a}_L^2 + \hat{a}_R^{\dagger 2} \hat{a}_R^2], \quad (4)$$

where we have introduced the time-dependent tunnelling energy

$$\Delta E(t) = \int_{-\infty}^{\infty} dy \varphi_L(y, d(t)) \left(-\frac{\hbar^2}{2M} \nabla^2 + V(y, d(t)) \right) \varphi_R(y, d(t)) = \hbar \omega \exp[-d^2(t)/\Delta y^2], \quad (5)$$

and $g = g_2 d_4$ with

$$d_4 = \int_{-\infty}^{\infty} dy \varphi_L^4(y, d(t)) = \frac{1}{2\sqrt{\pi} \Delta y}. \quad (6)$$

Note that we have neglected cross-phase modulation, consistently with the validity of the gaussian approximation in the description of the mode functions of the waveguide. We remark that this approximation only holds for $d > \Delta x$, otherwise the modes must be taken as time-dependent linear combinations of the energy eigenstates, a procedure requiring numerical diagonalization [6].

This two-mode problem is conveniently reexpressed in the Schwinger angular momentum representation of bosonic operators [29]. We proceed by introducing the angular momentum operators

$$\hat{J}_z = \frac{1}{2} (\hat{a}_L^\dagger \hat{a}_L - \hat{a}_R^\dagger \hat{a}_R), \quad (7)$$

$$\hat{J}_y = \frac{1}{2i} (\hat{a}_L^\dagger \hat{a}_R - \hat{a}_R^\dagger \hat{a}_L), \quad (8)$$

$$\hat{J}_x = \frac{1}{2} (\hat{a}_L^\dagger \hat{a}_R + \hat{a}_R^\dagger \hat{a}_L), \quad (9)$$

which can be thought of as the orthogonal components of a Bloch vector of length $N/2$. This corresponds to

mapping the quantum state onto a distribution on the Bloch sphere.

As usual, we then express the state of the matter-wave field in terms of eigenstates $|J, m\rangle$ of the operators \hat{J}^2 and \hat{J}_z , where

$$\hat{J}^2 = \hat{J}_x^2 + \hat{J}_y^2 + \hat{J}_z^2, \quad (10)$$

with

$$\begin{aligned} \hat{J}^2 |J, m\rangle &= \hbar^2 J(J+1) |J, m\rangle \\ \hat{J}_z |J, m\rangle &= \hbar m |J, m\rangle = \frac{\hbar}{2} (n_L - n_R) |J, m\rangle, \end{aligned} \quad (11)$$

and $J = N/2$, $m = -J, -J+1, \dots, J$.

In the angular momentum representation the Hamiltonian (4) reads

$$\hat{H} = f(J) + 2g \hat{J}_z^2 + \Delta E(t) \hat{J}_x, \quad (12)$$

where the energy $f(J)$ is a function of the total angular momentum eigenvalue J . For a fixed particle number, it yields a constant phase shift irrelevant for the problem at hand. The ground state of the Hamiltonian (12) is expressed in terms of the azimuthal quantum number

$$|\psi\rangle = \sum_{m=-J}^J c_m |J, m\rangle. \quad (13)$$

Each of the operators (7)-(9) generates rotations of this distribution around the corresponding axis. As seen from the Hamiltonian (12), and already proposed in Ref. [30] a rotation about the \hat{x} axis of the Bloch sphere can be achieved by turning on the quantum tunnelling between the two wells for a precisely determined time. As a result, it is possible to transform a number-squeezed state, characterized by reduced fluctuations in \hat{J}_z , into a phase-squeezed state, characterized by reduced fluctuations in \hat{J}_y . We exploit this feature of quantum tunnelling later on in to achieve sub-shot noise detection in the presence of repulsive interactions.

We mentioned that the detection of the atomic field is carried out after the optical waveguide is rapidly switched off and the atoms undergo a stage of ballistic expansion. The mode functions (3) no longer describe the spatial density of the condensate during that stage. Rather,

they must be replaced by free gaussians that are centered around the minima of the potential at the time of release

$$\varphi_{L/R}(y,t) = (2\pi\Delta y^2(1+i\omega t))^{-1/4} \times \exp\left(-\frac{(y\pm d)^2}{4\Delta y^2(1+i\omega t)}\right). \quad (14)$$

Taking the two halves of the condensate to have a relative phase Θ , the field operator for the ballistically expanding atoms becomes then

$$\hat{\Psi}(y,t,\Theta) = \hat{a}_L\varphi_L(y,t)\exp(i\Theta/2) + \hat{a}_R\varphi_R(y,t)\exp(-i\Theta/2), \quad (15)$$

resulting in the spatial density

$$\begin{aligned} \langle G_1(y,t,\Theta) \rangle &= \langle \hat{\Psi}^\dagger(y,t,\Theta)\hat{\Psi}(y,t,\Theta) \rangle = \frac{1}{\sqrt{2\pi\Delta y^2(1+\omega^2 t^2)}} \exp\left(-\frac{y^2+d(t)^2}{2\Delta y^2(1+\omega^2 t^2)}\right) \left[N \cosh\left(\frac{yd}{\Delta y^2(1+\omega^2 t^2)}\right) \right. \\ &\quad \left. + 2\langle \hat{J}_x \rangle \cos\left(\frac{yd}{\Delta y^2(1+\omega^2 t^2)}\omega t + \Theta\right) - 2\langle \hat{J}_y \rangle \sin\left(\frac{yd}{\Delta y^2(1+\omega^2 t^2)}\omega t + \Theta\right) \right]. \end{aligned} \quad (16)$$

The atomic density at any point in space and time is given by an incoherent contribution that is independent of both the relative phase and the internal dynamics of the two-mode condensate, as well as a coherent contribution.

Since the Hamiltonian \hat{H} is invariant with respect to the exchange $L \leftrightarrow R$, it is easily seen that for states symmetric with respect to the interchange of the two modes, $\langle \hat{J}_y \rangle = \langle \hat{J}_z \rangle = 0$ for all times, although $\langle \hat{J}_y^2 \rangle \neq 0$ as we discuss shortly. The coherent contribution to $\langle G_1(y,t,\Theta) \rangle$ is therefore proportional to the expectation value of $\langle \hat{J}_x \rangle$. In terms of the angular momentum picture, it can be interpreted as the polarization of the distribution. The visibility of the interference fringes of the ballistically expanding two-mode condensate,

$$V = \frac{\langle G_1(0,t,0) \rangle - \langle G_1(0,t,\pi) \rangle}{\langle G_1(0,t,0) \rangle + \langle G_1(0,t,\pi) \rangle} = \frac{|\langle \hat{J}_x \rangle|}{N/2}, \quad (17)$$

depends only on that expectation value, the associated fluctuations being given by

$$\begin{aligned} \Delta G_1 &\equiv \sqrt{\langle \Delta G_1^2(y,t,\Theta) \rangle} \\ &= \sqrt{\langle G_1^2(y,t,\Theta) \rangle - \langle G_1(y,t,\Theta) \rangle^2}. \end{aligned} \quad (18)$$

The phase resolution of atom-interferometric experiments is limited by the requirement that the change in local density resulting from an imprinted global phase change must be larger than the intrinsic fluctuations of

the first order correlation function

$$\Delta G_1 \geq \left| \frac{\partial \langle G_1 \rangle}{\partial \Theta} \right| \Delta \Theta. \quad (19)$$

This gives as an estimate for the phase resolution resulting from number fluctuations

$$\Delta \Theta = \frac{\sqrt{\langle \Delta G_1^2 \rangle}}{|\partial \langle G_1 \rangle / \partial \Theta|}. \quad (20)$$

Applying this criterion to the problem at hand, one finds that the phase resolution for the two-mode condensate is given by

$$\Delta \Theta^2 = \frac{\langle \hat{J}_y^2 \rangle}{\langle \hat{J}_x \rangle^2} + \frac{\langle \hat{N}^2 \rangle - \langle \hat{N} \rangle^2}{4\langle \hat{J}_x \rangle^2}. \quad (21)$$

The second term in Eq.(21) is equal to zero in an individual experimental event, but gives rise to a contribution of order unity if averaged over a classical (Poissonian) distribution of particle numbers in repeated experiments. The number of particles must therefore be determined with a high precision if one wishes to benefit from any enhancement of interferometric resolution due to phase squeezing. Setting this second term to zero for now, we recover the result derived by Kitagawa and Ueda in their seminal work on spin squeezing [31]. Squeezing along the \hat{y} -direction corresponds to increased correlations of the phases between the two wells, thus producing a better

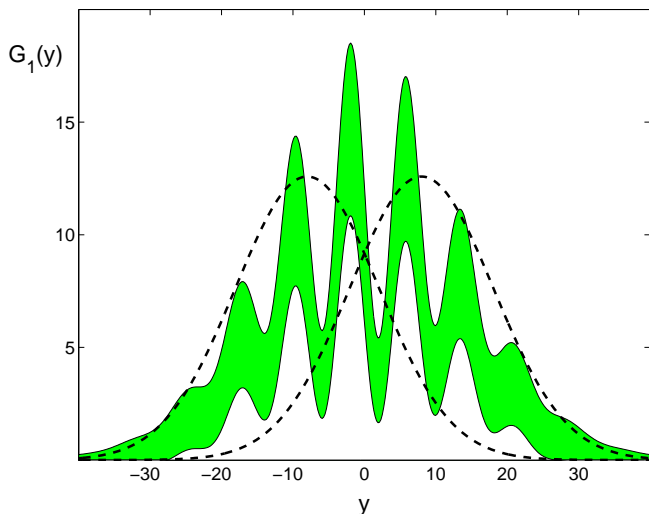


FIG. 1: Particle density bounded by density noise $\langle G_1 \rangle \pm \Delta G_1$ after ballistic expansion of a two-mode condensate with $N = 100$ in the ‘superfluid’ regime where the visibility is high. The dashed lines show the density of the mode functions. Transverse distance is measured in units of the oscillator width Δy and the initial condensates were centered around $d = \pm 8\Delta y$.

defined relative phase, a desirable feature in interferometric applications. The squeezing parameter, which we calculate relative to the standard quantum limit

$$\xi_y = \frac{\Delta\Theta}{\Delta\Theta_{SQL}} = \frac{\sqrt{N\langle \hat{j}_y^2 \rangle}}{\langle \hat{j}_x \rangle}, \quad (22)$$

although not necessarily representing the maximal achievable squeezing of the variances of the angular momentum distribution, was shown by these authors to represent the parameter of interest from the point of view of possible interferometric applications. Hence it is the major focus of the present study.

III. RESULTS

This section discusses the main results of our numerical study of the two-mode beam splitter. The analysis is based on the dimensionless parameter

$$G = \frac{2gN}{\Delta E}, \quad (23)$$

the ratio of mean-field energy to tunnelling energy, which completely determines the spectrum of the Hamiltonian.

Note however that the two-mode approximation implicitly assumes a stable condensate, a property that holds only for low enough densities in the case of attractive interactions [25].

We consider first the simple case of a static double-well system where the confining potential is suddenly turned-off, resulting into the formation of an interference

pattern after a period of ballistic expansion. The next subsection discusses the results of a full dynamical study.

A. Static double-well potential

The matter-wave interference pattern is shown in Fig. 1 in the superfluid regime, further illustrating the excellent contrast in that case. In addition to the fringe contrast, it is necessary to consider the quantum fluctuations of the interference pattern, since they lead to the fundamental limit in phase resolution of interferometric measurements. Figure 1 illustrates these fluctuations by attaching to the intensity $\langle G_1 \rangle$ a width given by twice its variance $\Delta G_1 = (\langle G_1^2 \rangle - \langle G_1 \rangle^2)^{1/2}$. We have seen in Eq. (21) that these fluctuations result in a phase resolution

$$\Delta\Theta^2 = \frac{\langle \hat{j}_y^2 \rangle}{\langle \hat{j}_x \rangle^2}, \quad (24)$$

where we have neglected the shot-to-shot number fluctuations for simplicity. The density noise is here proportional to $\sqrt{\langle G_1 \rangle}$, allowing at best for interferometry at the standard quantum limit.

Figures 2 and 3 shows the ground state distributions in terms of both the probability amplitudes $|c_m|$, and of the amplitudes $|c_{\theta_m}|$ of the ground state expressed on a basis of so-called relative phase states,

$$|\psi\rangle = \sum_m c_{\theta_m} |\theta_m\rangle, \quad (25)$$

where [32]

$$|\theta_m\rangle = \frac{1}{\sqrt{2J+1}} \sum_{m'=-J}^J \exp(im'\theta_m) |J, m'\rangle \quad (26)$$

and the discrete relative phases are given by

$$\theta_m = \theta_0 + \frac{2\pi m}{2J+1}, \quad (27)$$

for an arbitrary reference phase θ_0 chosen here to be zero.

For weak interactions, i.e. small $|G|$, the system is in a state reminiscent of a coherent state, with a relatively well defined phase with fluctuations consistent with the standard quantum limit. For large attractive interactions the ground state approaches a double peaked distribution, corresponding to a macroscopic superposition state as described in [26, 27]. For $G \ll -1$, the ground state can thus be approximated by

$$|\psi\rangle = \frac{1}{\sqrt{2}} [|J, J\rangle + |J, -J\rangle]. \quad (28)$$

This gives for the phase distribution

$$|\psi\rangle = \frac{1}{\sqrt{J+1/2}} \sum_{m=-J}^J \cos(J\theta_m) |\theta_m\rangle. \quad (29)$$

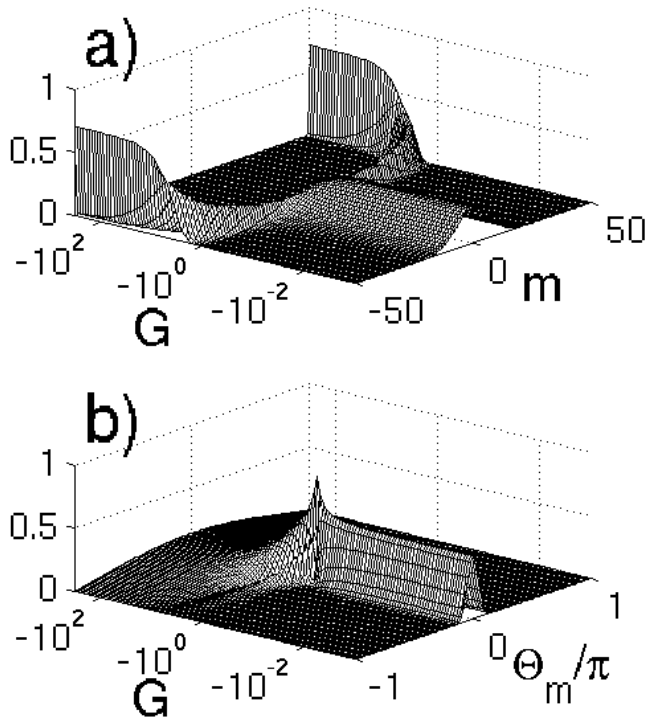


FIG. 2: Ground-state distributions as function of the dimensionless parameter G for attractive interaction. In a) magnitudes of ground state components $|c_m(G)|$ are shown for attractive interaction, and in b) the distribution of relative phase components $|c_{\theta_m}(G)|$ in Eq.(26).

The transition between the superfluid and superposition regimes takes place just below $G = -1$, where the relative phase becomes well defined due to squeezing.

For large repulsive interactions the ground state goes through the Mott-insulator transition in a continuous manner. Here the number distribution narrows and the phase distribution widens until it becomes essentially flat, indicating a completely random phase when averaged over an ensemble.

Figure 4 shows the uncertainties in the relative number $\Delta \hat{J}_z^2$, and the relative phase $\Delta \hat{J}_y^2$, together with their product $\Delta \hat{J}_y \Delta \hat{J}_z$ for $N = 100$ atoms. The uncertainty product is essentially constant in the region

$$-1 \ll G \ll \frac{1}{2}N^2, \quad (30)$$

where the upper limit was found from the simulations. In this interval the ground state resembles a coherent state, making this the superfluid regime. For large attractive interactions the uncertainty product increases at the superfluid-superposition transition and saturates for strong interactions. As the uncertainty in relative phase does not increase when compared to its value in the superfluid regime, the increase in the uncertainty product can be attributed solely to the increase in $\Delta \hat{J}_z$. The fact

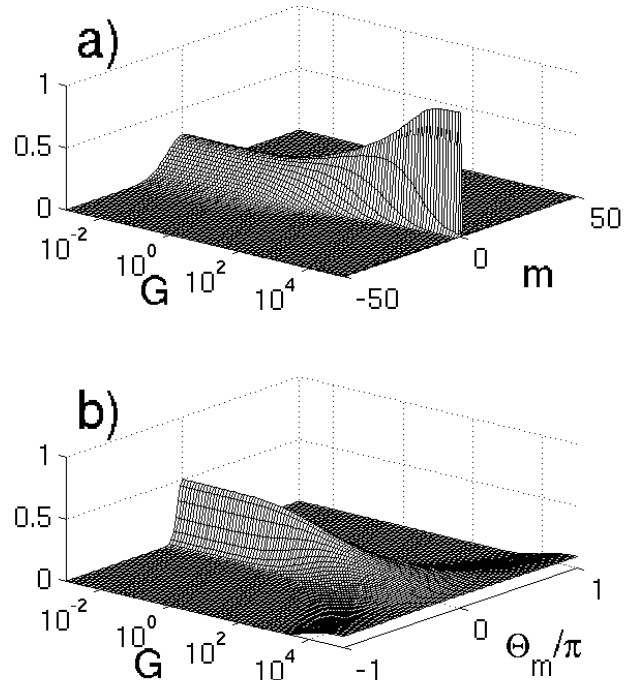


FIG. 3: Ground-state distributions as function of the dimensionless parameter G for repulsive interaction. In a) magnitudes of ground state components $|c_m(G)|$ are shown for attractive interaction, and in b) the distribution of relative phase components $|c_{\theta_m}(G)|$ in Eq.(26).

that the ground state in the superposition regime is double peaked, as can be seen in Fig. 2 and thus no longer a minimum uncertainty state, gives using Eq.(28) for the uncertainty in number difference

$$\langle \hat{J}_z^2 \rangle = J^2 = \frac{N^2}{4}, \quad (31)$$

in agreement with the numerical results, see for instance Fig. 4. On the Bloch-sphere the distribution is concentrated around the two regions $m = \pm J$, this bimodal character giving giving rise to a large spread in $\Delta \hat{J}_z$.

Figure 5 shows the visibility V of the fringes, Eq. (17), after the free expansion of the matter waves following the switching off of a static double-well potential. In case tunnelling dominates the dynamics of the system, we observe high-contrast interference fringes, but there is an abrupt transition, with contrast decreasing as $|G|^{-1}$ as soon as $G < -1$. The underlying physics governing the decrease of contrast is essentially the same as in the superfluid-Mott insulator transition predicted [23, 24] and observed in optical lattices [22]. If tunnelling dominates, the state of the two-mode system is essentially a superfluid with a well-established phase relationship between the two modes of the beam splitter, resulting in high-contrast interferences. In the superposition and

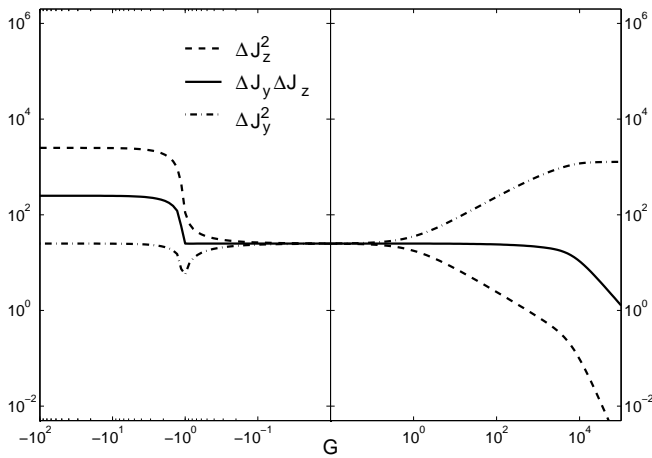


FIG. 4: The uncertainties $\Delta\hat{J}_y^2$, $\Delta\hat{J}_z^2$ and the product $\Delta\hat{J}_y\Delta\hat{J}_z$ as functions of G for $N = 100$. The phase uncertainty $\Delta\hat{J}_y^2$ goes through a global minimum at $G = -1$, the border between attractive superfluid and superposition states, and increases in the repulsive regime until it saturates to a constant value as the system passes through the Mott-insulator transition.

Mott regimes, by contrast, the two wells are isolated from each other, with no phase relationship between them.

This behavior of the fringe visibility can be further understood from the Heisenberg uncertainty relation

$$\Delta\hat{J}_y\Delta\hat{J}_z = \frac{1}{2}|\langle[\hat{J}_y, \hat{J}_z]\rangle| = \frac{1}{2}|\langle\hat{J}_x\rangle|, \quad (32)$$

which shows that the uncertainty product $\Delta\hat{J}_y\Delta\hat{J}_z$ is proportional to the polarization $\langle\hat{J}_x\rangle$ and thus the visibility (17). This shows that the regime of high visibility coincides with the one where uncertainty product is constant. This is, as expected, the superfluid regime. The polarization measures the coherence, here the degree to which adjacent wave function components c_m are populated. In the Mott-insulator and superposition regimes, the wave function becomes highly peaked around the center (minimal $|m\rangle$) and boundary (maximal $|m\rangle$) which thus limits the coherence.

In addition to illustrating that the visibility decreases outside the superfluid regime given by Eq. (30), Fig.5 also shows that for $G > 0$ and even particle number, the asymptotic value for the visibility is $V = \frac{1}{2}$ rather than zero for N odd. This difference in asymptotic behaviors can be explained as follows. For repulsive interactions and far into the Mott insulator regime, the ground state is approximately given by a Fock state with equal populations in both wells. In the case of odd atom number, the additional atom can be in either of the wells, so that

$$|\psi\rangle = \frac{1}{\sqrt{2}}\left[|J, \frac{1}{2}\rangle + |J, -\frac{1}{2}\rangle\right]. \quad (33)$$

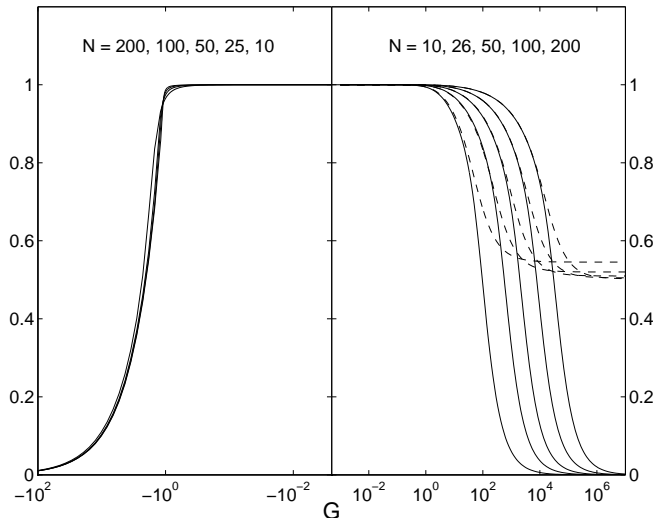


FIG. 5: Visibility of interference fringes for a ballistically expanding two-mode BEC as a function of G , the ratio between the mean-field and tunneling energies, for particle numbers ranging from 10 to 200. For attractive interaction the visibility decreases abruptly for $G < -1$. In the case of repulsive interaction the behavior is qualitatively and quantitatively different for even (solid) and odd (dashed) atom numbers, as explained in the text.

This gives for the polarization

$$\langle\hat{J}_x\rangle = \frac{1}{2}\left[J + \frac{1}{2}\right] \approx \frac{J}{2}, \quad (34)$$

and hence $V = 1/2$ as asymptotic value.

For the case of even particle number, in contrast, the asymptotic ground state for $G \rightarrow \infty$ is the Fock state $|m = 0\rangle$ with $N/2$ atoms in each well. For large but finite values of G the state can be approximated by

$$|\psi\rangle = \sqrt{1-2\varepsilon}|J, 0\rangle - \sqrt{\varepsilon}\left[|J, 1\rangle + |J, -1\rangle\right], \quad (35)$$

where epsilon is a small number. This gives for the polarization

$$\langle\hat{J}_x\rangle = 2\sqrt{\varepsilon}\sqrt{J(J+1)} \approx 2\sqrt{\varepsilon}J, \quad (36)$$

and an asymptotic value of the visibility $V \rightarrow 0$.

Let us now turn to the phase resolution $\Delta\Theta^2$ of the beam splitter. The left-hand side of Fig. 6 shows the variance $\Delta\Theta^2/\Delta\Theta_{\text{SQL}}^2$ after free ballistic expansion from the two-mode ground state of the beam splitter, plotted as a function of the ratio G between the mean field energy and tunnelling energy. The phase resolution exhibits a sharp minimum just below $G = -1$. At this point, we find numerically that the energy gap between the ground state and the first excited state of the double-well goes to zero within our numerical accuracy. This indicates the presence of a ‘quantum phase transition’ — or more precisely cross-over — a property also inferred

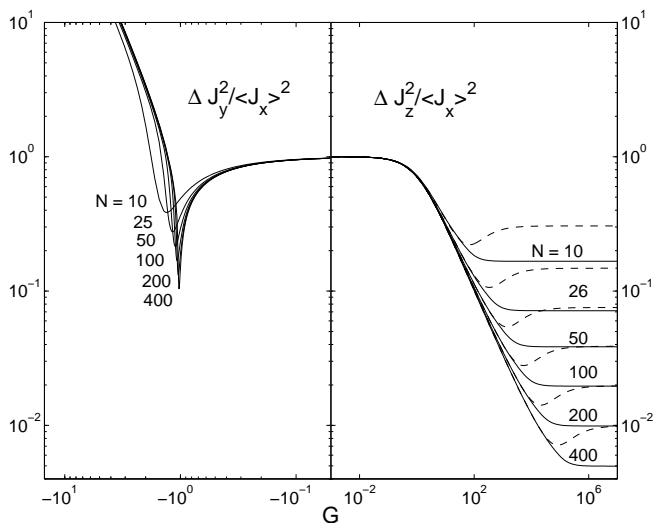


FIG. 6: Squeezing of the phase variance relative to the standard quantum limit for the two-mode ground state. For attractive interaction the phase squeezing is minimal just below $G = -1$. The crossover from Poissonian fluctuations in the superfluid regime $G < -1$ to the superposition state $G > -1$ becomes sharper with increased number of particles. For repulsive interaction there is a smooth transition between the superfluid regime of low G -values to the Mott-insulator state. In the asymptotic limit $G \rightarrow \infty$, the squeezing approaches a plateau, which is different for odd and even atom numbers.

from Fig. 2 where the quantum statistical properties of the ground state obviously change at the point $G = -1$. This transition is associated with the onset of increased number fluctuations between the populations of the two modes, and correspondingly to suppressed phase fluctuations. Hence, the phase resolution of the beam splitter is maximized at that point. As expected, the crossover from Poissonian fluctuations in the superfluid regime for $G > -1$ to a superposition state for $G < -1$ becomes sharper with increased particle number. For attractive interaction there is thus a squeezed state at the boundary between the superfluid and superposition regimes. For small atom numbers and attractive interaction, the minimum of $\Delta\Theta^2$ occurs to the right of the superfluid-superposition transition. From this discussion, it might appear favorable to operate the beam splitter in that regime. This is however misleading, as we must also take into account the fact that the fringe visibility rapidly decreases in that regime, as shown in Fig. 5. The situation improves rapidly for large N , though. The sharpness of the minimum, however, makes this state challenging to create experimentally in a controlled manner. In addition, the maximum achievable squeezing is limited due to the size limits imposed by the metastability of attractive condensates.

The situation is slightly more subtle in the case of repulsive interactions. From Fig. 2, it is quite clear that as the system moves into the Mott regime, the phase un-

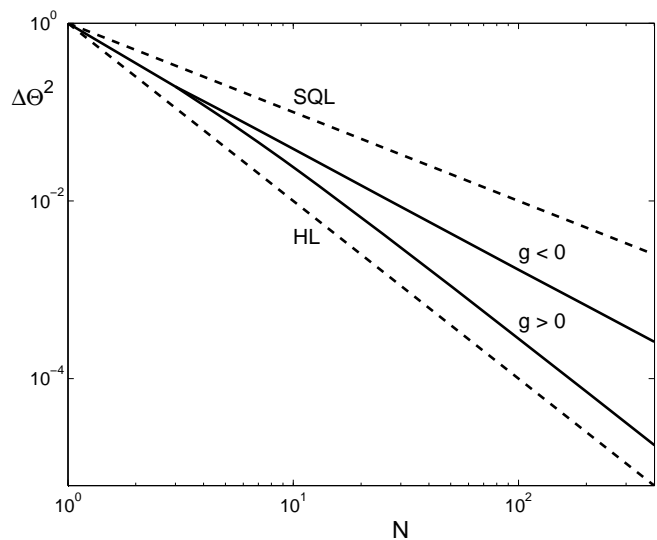


FIG. 7: Phase variance in the ground state of the double-well system at the “critical point” $G = -1$ for attractive condensates, and at $G = \frac{N^2}{2}$ for repulsive condensates, as functions of particle number. The dashed lines show the standard quantum limit (SQL) and Heisenberg limit (HL) for comparison.

certainty increases and the number fluctuations of the ground state become more strongly squeezed. This is also evidenced in Fig. 3, which shows the monotonic increase in $\Delta\hat{J}_y^2$ for increasing G . Hence, it would appear that the phase resolution becomes increasingly worse in this regime. This difficulty can however be eliminated by using quantum tunnelling to turn number squeezing into phase squeezing, as discussed in section II. As a result, the minimal obtainable phase fluctuations for $G > 0$ are given by

$$\Delta\Theta^2 = \frac{\Delta\hat{J}_z^2}{\langle\hat{J}_x\rangle^2} \quad (37)$$

since $\Delta\hat{J}_z = \langle\hat{J}_z^2\rangle$ is the minimal uncertainty of \hat{J}_z in deep the Mott regime. The right-hand side of Fig. 6 shows that the phase resolution achieved by this technique in the case of repulsive interactions. Just as for the visibility, we find here different asymptotic behavior for odd and even particle numbers with a factor of two in difference for large interactions. Using Eq.(33) we find for the uncertainty in number difference

$$\langle\hat{J}_z^2\rangle = \frac{1}{4}, \quad (38)$$

which together with Eq.(34) for the polarization gives

$$\frac{\langle\hat{J}_z^2\rangle}{\langle\hat{J}_x\rangle^2} \approx \frac{1}{J^2} = \frac{4}{N^2}, \quad (39)$$

in agreement with the asymptotic values for odd particle numbers, shown dashed in Fig. 6. For even numbers,

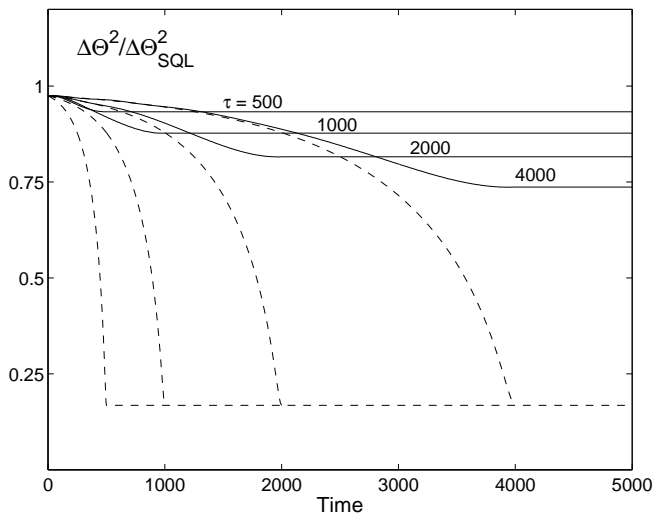


FIG. 8: Phase squeezing for $g < 0$ when $\Delta E(t)$ is taken to vary according to Eq.(42), for several values of the τ . The dashed lines show squeezing of the instantaneous ground state for comparison.

Eq.(35) yields

$$\langle \hat{J}_z^2 \rangle \approx 2\varepsilon, \quad (40)$$

which together with Eq.(36) gives

$$\frac{\langle \hat{J}_z^2 \rangle}{\langle \hat{J}_x \rangle^2} \approx \frac{1}{2J^2} = \frac{2}{N^2}, \quad (41)$$

in agreement with Fig.6. The behavior of both phase resolution and visibility for odd versus even particle numbers can thus be understood from the form of the ground state in the limit of large repulsive interactions.

Strictly speaking, $\Delta \hat{J}_y$ is the phase uncertainty only when the distribution spans an area narrower than the diameter of the Bloch sphere. For larger values the spread $\Delta \hat{J}_y$ behaves differently, as it is the projection onto the plane spanned by \hat{J}_y and \hat{J}_z , and not the distance along the equator. For the interferometric setup considered here the phase uncertainty is in general not equal to the phase resolution given by Eq. (21), as the latter will grow when the visibility goes down.

We have seen in Section II that the phase sensitivity of the system is closely related to spin squeezing. The squeezing of both optical and matter waves is of considerable interest in interferometry, as it offers the potential to beat the standard quantum limit of detection, and possibly replace it by the so-called Heisenberg limit scaling as $1/N$. Fig. 7 shows the phase variation of the ground state at both the “critical point” $G = -1$ for attractive interaction, and at $G = \frac{1}{2}N^2$ for repulsive interaction as functions of particle number N , the dashed lines giving the standard quantum limit (SQL) scaling as $1/\sqrt{N}$ and Heisenberg limit (HL) for comparison. The G-value

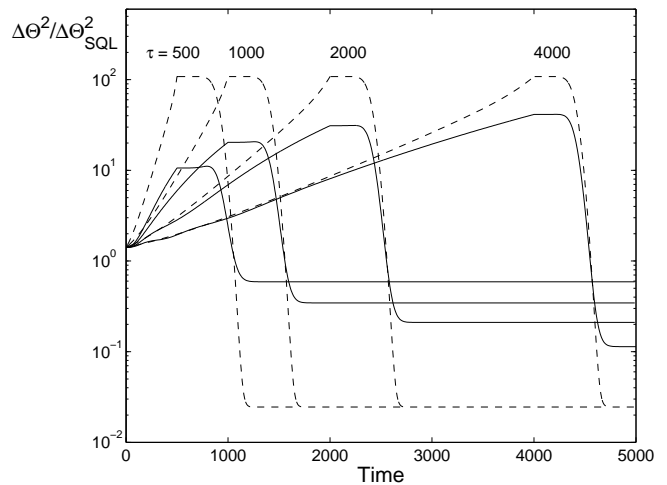


FIG. 9: Squeezing of the relative phase $\Delta\theta$ for a double well split in time according to equation Eq.(42).

in the repulsive regime was chosen to produce maximal squeezing for odd particle numbers, slightly worse than for even numbers. Since the particle number can not be controlled down to single units, this produces a conservative limit for the achievable squeezing.

The combination of the mean-field interaction and tunneling clearly leads to the squeezing of the matter-wave field and a sensitivity significantly improved from the standard quantum limit under the conditions mentioned above. We find numerically that for attractive interaction $\Delta\theta^2$ scales as $N^{-1.38}$, slightly above the asymptotic limit of $N^{-4/3}$ derived by Kitagawa and Ueda [31]. The difference is expected to decrease with increased particle number. For repulsive interaction we find $\Delta\theta^2 \propto N^{-2}$, thus corresponding to Heisenberg limited phase resolution. This comes at the price of larger interactions and also necessitates an additional rotation of the Bloch sphere.

B. Dynamics

The previous section investigated the ground state properties of the static double-well system. Here we discuss ways to create states with the desired properties starting from a condensate in the ground state with a small interwell separation. The adiabatic theorem of quantum mechanics states that a system governed by a time dependent Hamiltonian and initially prepared in an eigenstate will remain in the instantaneous eigenstate given that the Hamiltonian changes sufficiently slowly. The aim here is evolve the system adiabatically [33] into states of maximal squeezing and then freeze the dynamics.

Controlling the magnitude and sign of two-body interaction is readily achievable using Feshbach resonances. The rate at which the magnetic field can be swept across a resonance is much higher than typical trap frequencies

and tunnelling rates, allowing for a practically instantaneous switching of the nonlinear interaction. Decreasing the tunnelling rate can be achieved by rapidly separating the two wells as the point of minimal phase fluctuations is reached.

We model the splitting of the symmetric double-well potential using a tunnelling potential $\Delta E(t)$ that decreases exponentially in time

$$\Delta E(t) = \hbar\omega \exp\left(-\frac{d_{\min}^2}{\Delta y^2} - \Gamma t\right), \quad (42)$$

where d_{\min} is the minimal separation between the wells, and the constant Γ is a measure of how fast the wells are separated. The separation is assumed to occur over a finite time τ and to reaching a value $d(\tau)$ such that $G = -1$ for attractive interaction, and $G = \frac{1}{2}N^2$ for repulsive interaction. The constant Γ is adjusted accordingly. As the time $t = \tau$ is reached, the two-body interaction is rapidly taken to zero to freeze the dynamics.

The evolution after $t = \tau$ is linear and solely governed by tunnelling. Note that for attractive interactions, the residual rotation of the distribution resulting from quantum tunnelling has to be kept small in order to avoid transforming the phase squeezing into number squeezing,

$$\int_{\tau}^{\infty} \Delta E(t) dt \ll \hbar\pi, \quad (43)$$

This can be achieved by either taking $\Delta E(\tau) \ll 1$ at the point where $G = -1$, or separating the wells rapidly after $t = \tau$ to make the left-hand side of Eq. (43) negligible.

The squeezing in the phase variation for attractive interaction is shown versus time in Fig. 8 for several values of the parameter τ . The instantaneous squeezing of the true ground state is shown dashed for comparison. The evolution of the system is initially adiabatic, but becomes diabatic for larger separations making the system freeze out in a state less squeezed than the desired ground state. Longer evolution times make the system more adiabatic thus achieving squeezing closer to, but still far from the optimal values. For all cases shown in Fig. 8 it is however apparent that the dynamics is only partially adiabatic and that the minimal phase variation is severely limited by violation of the requirement that the dynamics be adiabatic.

Figure 9 shows the squeezing dynamics of a condensate with repulsive interaction when the tunnelling energy is decreased exponentially in time according to Eq.(42). As the value $G = \frac{1}{2}N^2$ is reached, the two-body interaction is rapidly tuned to zero. After that a pulse of tunnelling interaction, which corresponds to bringing the two wells closer again, is applied in such a way that

$$\int_{\tau}^{\infty} \Delta E(t) dt = \frac{\hbar\pi}{2}, \quad (44)$$

thereby rotating the Bloch-sphere distribution by an angle $\pi/2$ around the \hat{J}_x -axis and thus transforming the

number squeezing into phase squeezing without otherwise changing the distributions.

Initially the phase variance is seen to increase as the state becomes number-squeezed for increasing values of $G(t)$ until the time $t = \tau$ is reached when $g \rightarrow 0$, effectively freezing the evolution until the tunnelling pulse (44) is applied. For all values of τ , which are indicated in Fig.9, the same tunnelling pulse was used. The dynamics is seen in Fig. 9 to become more and more adiabatic as the value of τ is increased, just as in the case of attractive interaction. Here, however, the maximal squeezing achieved is larger than for the attractive case. This is not obvious at first, even though the repulsive ground state is more squeezed, as the system has to be evolved to values of stronger interaction than in the attractive case.

IV. CONCLUSION AND OUTLOOK

In this paper we have investigated the full quantum dynamics of a condensate in a symmetrically split double well. Expressions for the visibility and phase resolution during a ballistic expansion stage were given and investigated numerically. The possibility of creating phase squeezed ground states by adiabatic splitting was demonstrated, but is limited by the time scales involved. The increased phase sensitivity for ground states of attractive condensates, which are known to be stable only for particle numbers [25] up to around $N \approx 10^3$, was found to require long splitting times to achieve adiabatic evolution. For repulsive condensates where the densities are limited only by the requirement that the two-mode model be applicable, a scheme with scaling at the Heisenberg limit was outlined and tested in dynamics simulations. The original Heisenberg-limited scheme suggested in [16] for optical MZ interferometers and later applied in various forms to the case of atomic condensates [17, 18, 19], used dual Fock-states. i.e. the state was of the form given by Eq.(35). In the present context such states are unsuitable due to their low visibility. The problems can be avoided by not taking the system deep into the Mott-insulator regime where the ground state is the dual Fock state, but rather to the threshold where $G = N^2/2$, and the visibility still is high.

It is well known that the introduction of a linear potential, for instance due to gravity, changes the localization properties of the double-well eigenfunctions. The corresponding effects in the many-body regime are presently explored experimentally [34] and will also be the subject of future theoretical investigations.

Acknowledgments

This work is supported in part by the US Office of Naval Research, by the National Science Foundation, by the US Army Research Office, by the National Aeronautics and Space Administration, and by the Joint Services

-
- [1] G. Birkel, F. B. J. Buchkremer, R. Dumke, W. Ertmer, *Opt. Comm.* **191**, 67 (2001).
- [2] J. Reichel, *Appl. Phys. B* **75**, 469 (2002).
- [3] D. Müller, E. A. Cornell, M. Prevedelli, P. D. D. Schwindt, A. Zozulya, and D. Z. Anderson, *Opt. Lett.* **25**, 1392 (2000).
- [4] D. Cassettari, B. Hessmo, R. Folman, T. Maier, J. Schmiedmayer, *Phys. Rev. Lett.* **85**, 5483 (2000).
- [5] R. Dumke, T. Mütter, M. Volk, W. Ertmer, and G. Birkel, *Phys. Rev. Lett.* **89**, 220402 (2002).
- [6] M. Jääskeläinen, and S. Stenholm, *Phys. Rev. A* **68**, 033607 (2003).
- [7] L. A. Collins, L. Pezzé, A. Smerzi, G. P. Berman, and A. R. Bishop, [quant-th/0404149](https://arxiv.org/abs/quant-th/0404149).
- [8] E. A. Hinds, C. J. Vale, and M. G. Boshier, *Phys. Rev. Lett.* **86**, 1462 (2001).
- [9] E. Andersson, T. Calarco, R. Folman, M. Andersson, B. Hessmo, and J. Schmiedmayer, *Phys. Rev. Lett.* **88**, 100401 (2002).
- [10] O. Zobay, and B. M. Garraway, *Opt. Comm.* **178**, 93 (2000).
- [11] M. D. Girardeau, K. K. Das, and, E. M. Wright, *Phys. Rev. A* **66**, 023604 (2002).
- [12] D. C. E. Bortolotti, and, J. L. Bohn, *Phys. Rev. A* **69**, 033607 (2004).
- [13] J. A. Stickney, and A. A. Zozulya, *Phys. Rev. A* **68**, 013611 (2003).
- [14] C. P. Search, and P. Meystre, *Phys. Rev. A* **67**, 061601 (2003).
- [15] D. J. Wineland, J. J. Bolinger, W. M. Itano, F. L. Moore, and D. J. Heinzen, *Phys. Rev. A* **46**, R6797 (1992).
- [16] M. J. Holland and K. Burnett, *Phys. Rev. Lett.* **71**, 1355 (1993).
- [17] P. Boyer and M. Kasevich, *Phys. Rev. A* **56**, R1083 (1997).
- [18] J. A. Dunningham and K. Burnett, *Phys. Rev. A* **61**, 065601 (2000).
- [19] J. A. Dunningham, K. Burnett, and S. M. Barnett, *Phys. Rev. Lett.* **89**, 150401 (2002).
- [20] C. C. Gerry and R. A. Campos, *Phys. Rev. A* **68**, 025602 (2003).
- [21] C. Orzel, A. K. Truchman, M. L. Fenselau, and M. A. Kasevich, *Science* **291**, 2386 (2001).
- [22] M. Greiner, O. Mandel, T. Esslinger, T. W. Hänsch, and I. Bloch, *Nature* **415**, 39 (2002).
- [23] M. P. A. Fisher, P. B. Weichman, G. Grinstein, and D. S. Fisher, *Phys. Rev. B* **40**, 546 (1989).
- [24] D. Jaksch, C. Bruder, J. I. Cirac, C. W. Gardiner, and P. Zoller, *Phys. Rev. Lett.* **81**, 3108 (1998).
- [25] P. A. Ruprecht, M. J. Holland, K. Burnett, and M. Edwards, *Phys. Rev. A* **51**, 4704 (1995); G. Baym, and C. Pethick, *Phys. Rev. Lett.* **76**, 6 (1996); Y. Kagan, G. V. Shlyapnikov, and J. T. M. Walraven, *Phys. Rev. Lett.* **76**, 2670 (1996).
- [26] M. Steel and M. Collett, *Phys. Rev. A* **57**, 2920 (1998).
- [27] J. I. Cirac, M. Lewenstein, K. Mølmer, and P. Zoller, *Phys. Rev. A* **57**, 2920 (1998).
- [28] Y. Shin, M. Saba, T. A. Pasquini, W. Ketterle, D. Pritchard, and A. E. Leanhardt, *Phys. Rev. Lett.* **92**, 050405 (2004).
- [29] G. J. Milburn, J. Corney, E. M. Wright, and D. F. Walls, *Phys. Rev. A* **55**, 4318 (1997).
- [30] J. F. Coburn, G. J. Milburn, and W. Zhang, *Phys. Rev. A* **59**, 4630 (1999).
- [31] M. Kitagawa, and M. Ueda, *Phys. Rev. A* **47**, 5138 (1993).
- [32] D. T. Pegg and S. M. Barnett, *Phys. Rev. A* **39**, 1665 (1989); A. Luis and L. L. Sanchez-Soto, *Phys. Rev. A* **48**, 4702 (1993).
- [33] J. Javanainen and M. Yu, Ivanov, *Phys. Rev. A* **60**, 2351 (1999).
- [34] M. Kasevich, private communication.